In situ and satellite long-term monitoring of two earthflows of the Italian southern Apennines and of the structures built on them

Roberto Vassallo,* Jacopo De Rosa,* Caterina Di Maio,*
Diego Reale,** Simona Verde,** Gianfranco Fornaro**

Summary

This paper reports the results of a long-term monitoring of the slow movements of two deep earthflows in tectonized clay shales of southern Apennines. The cumulated movements have caused over the years severe damage to buildings and infrastructure, with important social and economic costs. Deep and superficial displacements, along with pore water pressures, are being monitored since 2005; in some areas of the slope, displacement monitoring by inclinometers started about 30 years ago. The kinematics of the landslides has been clarified sufficiently on the basis of ground-based measurements. On the other hand, the mostly N-S orientation of displacements, and the rather limited urbanization, make it rather challenging to monitor the area by satellite interferometry methodology. To minimize such problem, satellite data relative to areas where the displacements and their directions are clearly determined by inclinometers and GPS were analysed at the most detailed scale of analysis. The data validation allowed to confidently exploit remote sensing results in a wider area. Thus, images acquired by the COSMO-SkyMed satellite system, supplemented by ERS and Envisat data (available since 1993), allowed the reconstruction of the kinematic history of the urbanized area even where inclinometer displacement series were available only over short periods. Indications about the effectiveness of the remedial measures constructed in the area under study could also be obtained.

1. Introduction

Structurally complex clayey formations outcropping in the Italian Apennines are extensively affected by large landslides, from slow to extremely slow, which cause damage to buildings, tunnels, bridges, railways, highways and pipelines that are built on or across them, with consequent important social and economic costs [Mansour *et al.*, 2011; Corominas *et al.*, 2014; Turner, 2018; Ferlisi *et al.*, 2019; Picarelli *et al.*, 2021]. Due to their extension and to the mechanical behaviour of the involved materials, generally prone to deterioration [Picarelli and Russo, 2004; Picarelli and Di Maio, 2010], risk mitigation is generally difficult and requires intensive investigation. Monitoring of deep displacements and internal deformations of the landslide masses is fundamental for the comprehension of their kinematics and the design of possible remedial measures [Picarelli, 2007; Glastonbury and Fell, 2008; Cascini *et al.*, 2014; Kavoura *et al.,* 2020; Di Maio *et al.,* 2020]. While deep displacements and internal deformations can only be evaluated by in situ measurements, superficial displacements can also be evaluated by remote sensing. In this context, the interferometric processing of data acquired by satellite Synthetic Aperture Radar (SAR) reveals to be a useful tool, allowing to monitor all the elements that act as permanent scatterers, *i.e.*, that are characterized by an electromagnetic response coherent over all the observation period [Fornaro *et al.*, 2014; Noviello *et al.*, 2020; Peduto *et al.*, 2020].

Ground-based monitoring data are directly comparable to remote sensing data, for validation purposes, when clear evidence of the displacement direction is available (*e.g.,* Calò *et al.*, 2014; Bovenga *et al.*, 2017; Di Maio *et al.*, 2018). More generally, instead, integration between independent ground- and satellite-derived data is possible, for both wide-area investigations and local analyses [Refice *et al.*, 2019]. The advantages of the SAR technique, such as cost effectiveness, accuracy, high density of monitored scatterers and use of "natural targets", have been broadly checked and recognized (*e.g.* Colesanti and Wasowski, 2006; Herrera *et al.*, 2013; Journault *et al.*, 2018). Furthermore, the availability of long satellite data series makes it possible to improve the detection of landslide boundaries, analyze the history of movements and even the influence of remedial measures [Bru *et al.*, 2017; Di Maio *et al.*, 2018; Confuorto *et al.*, 2019]. Monitoring via the SAR technique has been proven effective even to design long-term stabilization works, verifying the results progressively achieved by the observational

* School of Engineering, University of Basilicata, Potenza, Italy
** Institute for Electromagnetic Sensing of the Environment, National Research Council (CNR-IREA), Napoli, Italy

 dx.doi.org/10.19199/2021.4.0557-1405.077

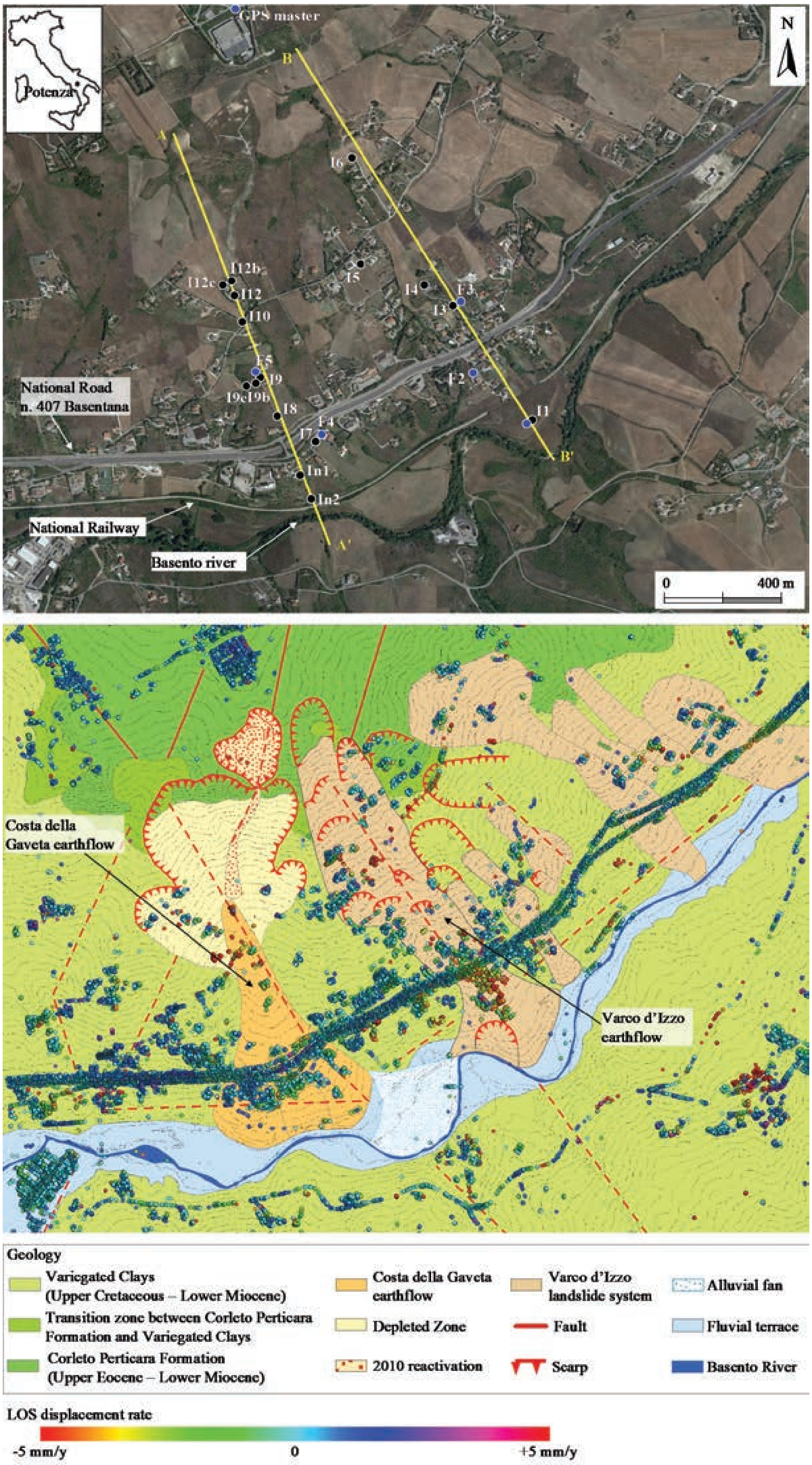

Fig. 1 – Study area with location of inclinometers and GPS stations (superimposed to a Google Earth view – Landsat/Copernicus image) a); geological-geomorphological map of *Costa della Gaveta* and *Varco d'Izzo* landslide systems (redrawn from VASSALLO *et al.*, 2020) with LOS average displacement rates from CSK data b).

Fig. 1 – Area di studio con indicazione della posizione degli inclinometri e delle stazioni GPS (base: Google Earth – immagine Landsat/Copernicus) a); carta geologica-geomorfologica dei sistemi franosi di Costa della Gaveta e Varco d'Izzo (ridisegnata da VASSALLO et al.*, 2020) con indicazione delle velocità media lungo la LOS da dati CSK b).*

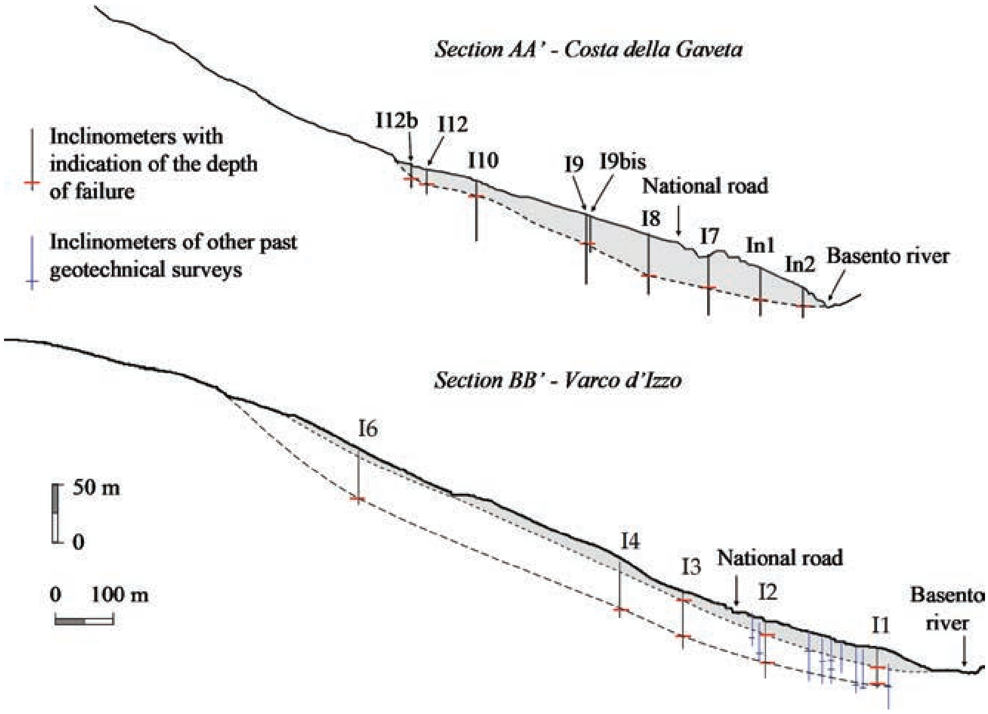

Fig. 2 – Longitudinal sections of *Costa della Gaveta* and *Varco d'Izzo* main earthflows with indication of slip surfaces reconstructed from inclinometer data (redrawn from VASSALLO *et al.*, 2020).

Fig. 2 – Sezioni longitudinali delle colate principali di Costa della Gaveta e Varco d'Izzo con indicazione delle superfici di scorrimento ricostruite sulla base delle misure inclinometriche (ridisegnate da VASSALLO et al.*, 2020).*

method [FERRIGNO *et al.*, 2015]. It can help to identify the causes of persistent damage to buildings [HANDWERGER *et al.*, 2013; NIKOLAEVA *et al.*, 2014; ANTRONICO *et al.*, 2015; FERRIGNO *et al.*, 2015; CROSTA *et al.*, 2017; BORRELLI *et al.*, 2018; INFANTE *et al.*, 2019] and transport infrastructure. This latter, in the case of non urbanized landslides, is frequently the main element visible by the satellites that allows to reconstruct the movement pattern when limited instrumentation for ground-based monitoring is available [WASOWSKI and BOVENGA, 2014; NORTH *et al.*, 2017; NAPPO *et al.*, 2019; FERLISI *et al.*, 2021].

The case study of the *Costa della Gaveta* slope (Potenza, Italy, Figs. 1 and 2) is particularly suitable for testing the integration of different monitoring techniques. As a matter of fact, with more or less continuity, inclinometer data are available for the last 30 years, and continuous inclinometer and GPS data are available for the last 15 years [DI MAIO *et al.*, 2010; CALCATERRA *et al.*, 2012; DI MAIO *et al.*, 2013; DI MAIO *et al.*, 2017; VASSALLO *et al.*, 2020]. The landslide systems of the slope show significant variations in displacement rates from a zone to another, ranging from very to extremely slow moving, due to their articulated geometry and local conditions.

The integration of directly measured displacement data with satellite multipass Differential Interferometric SAR (DInSAR) data, which has already been experimented in this area over a limited period of time [VASSALLO *et al.*, 2020], has great potential to add information fundamental to understand and predict the behaviour of the landslides, by examining broader areas. This potential is already evident from the distribution of displacement rates along the satellite Line Of Sight (LOS) superimposed to the geological-geomorphological map of the *Costa della Gaveta* and *Varco d'Izzo* landslide systems (Fig. 1b). The availability of long and robust series of ground-based displacement data allows for an appropriate use of DInSAR data which, for the case under study, would otherwise not be easily interpretable. This is because the direction of displacements, close to N-S, implies their mapping into a small component along the LOS.

The aim of this study is to identify the best procedure for increasing the density of information relative to the displacement field and its evolution in time by the use of satellite data, in order to have a deeper insight in the landslide kinematics and the effectiveness of remedial measures realized in the investigated area.

2. Study area

The study area is located at the eastern suburbs of the city of Potenza. The geological and geomorphologic features of *Costa della Gaveta* hill were investigated by DI MAIO *et al.* [2010] and VASSALLO *et al.* [2016; 2020]. The slope facing the Basento river is affected by several landslides crossed by a National Road and the National Railway (Fig. 1), the most important of which, *i.e.* the homonymous *Costa della Gaveta* earthflow and the *Varco Izzo* earthflow, are here the major focus of analysis. The formation mainly involved, Variegated Clays (Upper Cretaceous – Lower Miocene), is constituted by tectonized clays and clay marls. The landslides also incorporate rock fragments, blocks, and disarranged strata of marly limestone and calcarenite of the overlying Corleto Perticara formation (Eocene–Oligocene). The two landslides have been extensively studied in the last 15 years and monitored by GPS stations for continuous and periodic measurements, and ground-based devices, including a large number of mobile and fixed-in-place inclinometers, distributed fibre-optic strain sensors, along with piezometers, total stress cells and other systems specific for the chemical characterization of the pore fluid [DI MAIO *et al.*, 2010; CALCATERRA *et al.*, 2012; DI MAIO *et al.*, 2013; VASSALLO *et al.*, 2015; DI MAIO *et al.*, 2015; DI MAIO *et al.*, 2017; MINARDO *et al.*, 2018; VASSALLO *et al.*, 2020]. The number of instrumented boreholes has increased over the years. Displacement data were recorded over time spans different from zone to zone, depending on the local velocities, until the inclinometer tubes have gone out of use for excessive shearing. In several cases, the tubes out of use have been replaced by new ones. In some areas of the slope, further data of inclinometers installed by different public or private agencies are available since 1993, although each system has been working over only a few years. The monitoring results, as a whole, allowed to reconstruct the geometry of the main slip surfaces (Fig. 2) and the main kinematic features of the earthflows [VASSALLO *et al.*, 2020].

3. Ground-based and GPS displacement monitoring

The time series of the basal and superficial displacements of *Costa della Gaveta* earthflow are reported by figures 3a and 3b, respectively. The two sets of data are quite similar, because the contribution of the deformations internal to the landslide body are limited [VASSALLO *et al.*, 2020]. In other words, concentrated sliding along a thin slip band is the prevailing movement, consistently with the data reported in the literature for the slow/extremely slow stage of this type of landslides [GUIDA and IACCARINO, 1991; HUNGR *et al.*, 2014; URCIUOLI *et al.*, 2016]. Every time series shows an almost linear trend, with an average slope, *i.e.*, an average displacement rate, that decreases in the downslope direction. Such decrease has been interpreted as the result of a constant soil discharge mechanism [DI MAIO *et al.*, 2010; DI MAIO *et al.*, 2013]. Seasonal variations of deep displacement rates are linked to rainfall-induced pore water pressure changes in the slip zone [DI MAIO *et al.*, 2020; DI MAIO *et al.*, 2021]. Figure 3b also shows that, in the landslide main track, GPS8 extends the displacement information of inclinometer I8 that went out of use in 2013 [VASSALLO *et al.*, 2020]. The most recently installed inclinometer I9bis results in substantial continuity with the nearby inclinometers I9 and I9b. In the lateral sector of the depositional area (*i.e.*, the accumulation), inclinometer I7 has shown a very regular trend over 16 years, with displacement rates in the order of less than 1 mm/year. In the central sector of the accumulation, it will be shown that satellite data indicate slightly higher rates than I7, in the order of a few mm/year.

As for the *Varco d'Izzo* earthflow, inclinometer profiles indicate two main slip surfaces (Fig. 2), significant internal deformations, and displacement rates higher that those of the *Costa della Gaveta* earthflow. The displacements along the shear bands and the superficial ones are reported in figure 3c, which shows the significant heterogeneity of time rates from a zone to another of the landslide body. In the same figures, the results of GPS measurements of the two permanent stations F1 and F3 [CALCATERRA *et al.*, 2012; VASSALLO *et al.*, 2020] are also plotted, so as to extend the displacement data of inclinometers I1 and I3 until 2020. Also in this case, displacement series can be considered substantially linear in the period 2005-2020.

4. Satellite Multipass DInSAR displacement monitoring

As it is well known, DInSAR measurements provide the component of the displacements along the radar LOS that, for current SAR satellite systems, is typically oriented in the West-East direction with and incidence angle, *i.e.* the angle of the radar pointing direction with respect to the vertical, ranging from about 20° to 50°, depending on the sensor and the imaging mode. Consequently, the sensitivity to North-South displacement components is quite small [CASCINI *et al.*, 2010]. The displacement direction at *Costa della Gaveta* (Fig. 1) is such as to provide a small component along the LOS, often in the order of magnitude of the measurement error.

The DInSAR data considered in this paper are relative to ERS, Envisat and COSMO-SkyMed sensors (this latter is indicated as CSK in the following). ERS data (1992-2000), and Envisat data (2003 – 2010), acquired respectively on descending and ascending passes of the satellite, are those processed within the Italian *PST-A* (*i.e.* High Precision Not-Ordinary Plan of Remote Sensing, COSTANTINI *et al.*, 2017). The

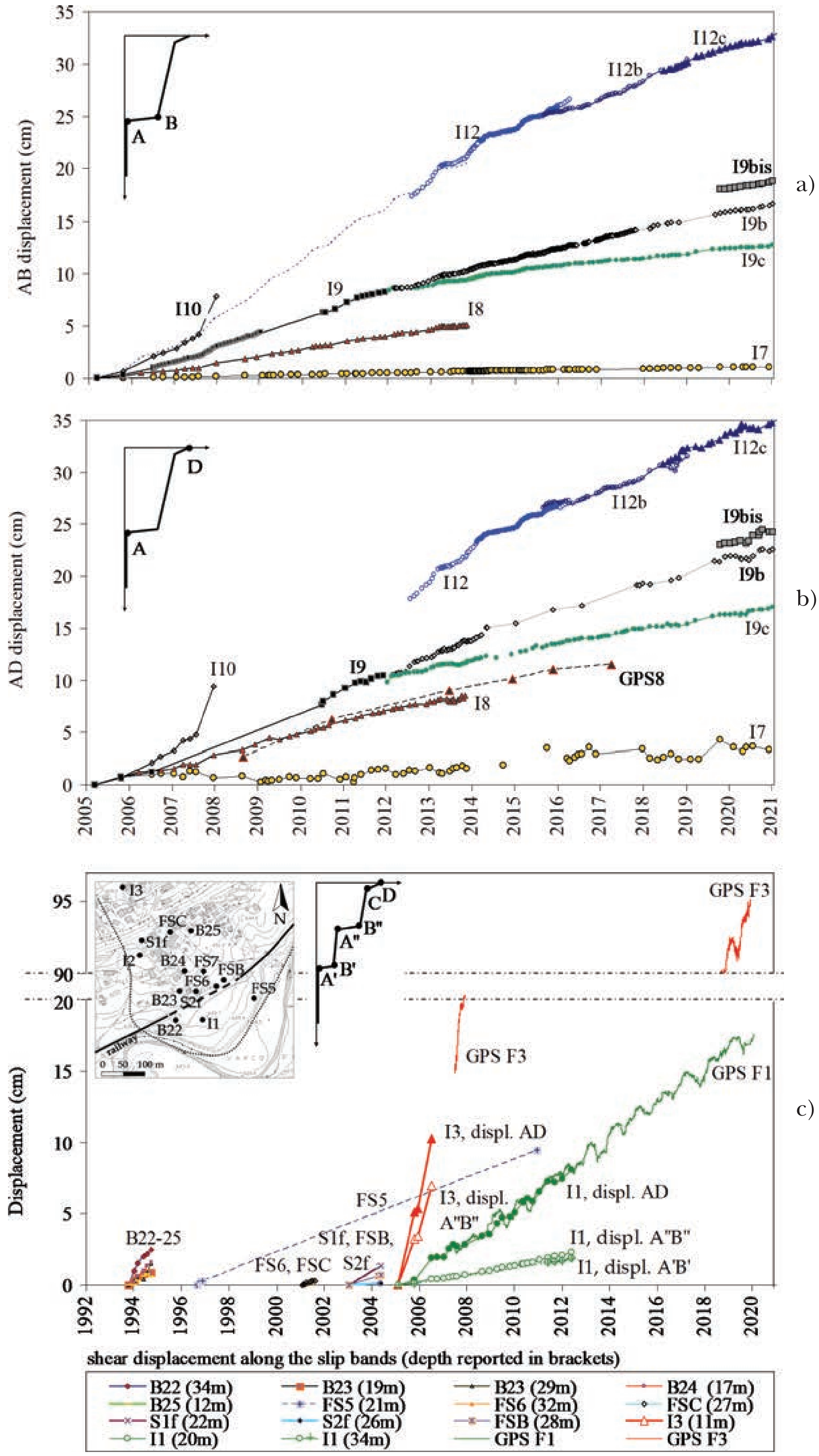

Fig. 3 – Time series of basal a) and superficial b) displacements of *Costa della Gaveta* earthflow, and basal and superficial displacements c) of *Varco d'Izzo* earthflow, evaluated by inclinometer and GPS measurements (redrawn from VASSALLO *et al.*, 2020, and updated).

Fig. 3 – Serie temporali degli spostamenti basali a) e superficiali b) della colata di Costa della Gaveta, e degli spostamenti basali e superficiali c) della colata di Varco d'Izzo, valutati tramite misure inclinometriche e GPS (ridisegnati da VASSALLO et al., *2020 e aggiornati).*

number of ERS scatterers is extremely limited for the studied slope, therefore their data were considered only for the few points showing unambiguous time trends. CSK ascending data were provided by the Italian Space Agency (ASI).

The CSK dataset, composed by 100 images acquired in the H-Image mode in the period 2012 - 2020, was processed through the SAR Tomography technique [FORNARO *et al.*, 2014, NOVIELLO *et al.*, 2020]. Similarly to Persistent Scatterer Interferometry (PSI), SAR Tomography is tailored to the processing of multipass SAR data at the full available spatial resolution for the analysis of the Persistent Scatterers (PS), *i.e.* ground targets which are concentrated in space (with respect to the wavelength and spatial resolution) and whose electromagnetic response is sufficiently coherent over all the observation period. SAR Tomography performs the imaging of the electromagnetic backscattered profile in a multi-dimensional domain given by space, time, and possibly temperatures. Theoretical analysis carried out in the framework of the detection theory proves that SAR tomographic methods allow reaching the best performances in terms of detection of PS [DE MAIO *et al.*, 2009].

Specifically, the data have been processed by the two-scale processing method [FORNARO *et al.*, 2014]. Low resolution processing with a Small Baseline Subset (SBAS) DInSAR algorithm was first used to retrieve the small scale deformation and atmospheric phase propagation delay (APD) on almost all the frame (40km x 40km) at a coarser resolution. The subsequent high resolution tomographic processing allowed zooming in on the specific sites of interest thus providing the large scale products at the highest available spatial resolution. The second stage was carried out on data calibrated for the APD and small scale deformation estimated at coarser resolution. It was implemented through the procedure reported by FORNARO *et al.* [2009] and FORNARO *et al.* [2014], based on the exploitation of a filter measuring the correlation of the acquired data with the expected phase model accounting for the parameters of interest (elevation and velocity). The detection of the output measurement points was implemented through the decision test in DE MAIO *et al.* [2009], corresponding to the Generalized Likelihood Ratio Test (GLRT) and essentially given by a comparison of the normalized output of the Beamforming filter, *i.e.* the tomographic coherence, with a given threshold.

Average displacement rates along the LOS (v_{LOS}) are reported for the *Costa della Gaveta* and the *Varco d'Izzo* earthflows in figures 4a-b and 4c-d, respectively. The rate values, calculated on the basis of the variation in the distance ΔS between the satellite and the scatterers, are the slopes of the ΔS-time series in the observation period. The capability of the CSK sensor to detect, thanks to the high resolution, the details of the spatial variability of the measurements is quite evident by the large difference in the density of visible scatterers between Envisat and CSK data. As expected, in both cases, most scatterers are located in correspondence of buildings or roads. A large number of scatterers is visible along the National Road, especially for the CSK data. Urbanization of the study area is anyway limited, and this poses a challenge to push forward the use of interferometric techniques for displacement monitoring.

As for the displacement time series along the LOS deriving from the processing of CSK data, among the buildings of the landslide areas, 21 main targets have been identified within the *Costa della Gaveta* earthflow and 35 main targets have been identified within the *Varco d'Izzo* earthflow (Fig. 5). By setting the minimum threshold of 0.5 mm/year for the velocity along the LOS as an indicator of movement [CASCINI *et al.*, 2013; PEDUTO *et al.*, 2015], a number of displacing targets, equal to 14 and 24 respectively, is detected, rather well distributed over the two landslides. The figure reports for some representative targets the displacement time series, that can all be considered fundamentally linear. The number of points detectable on each building is such that a range of displacement time series is obtained. The statistical distribution of the average yearly rates of such time series is also reported. The order of magnitude of the observed rates, that as mentioned above represent a small component of the total displacement rates, is from 1 to 10 mm/year.

5. Interpretation of remote sensing data in the areas with the largest ground-based information

To obtain the horizontal component of displacements from the described data, the procedure illustrated by DI MAIO *et al.* [2018] was used, based on trigonometric calculations considering:

- orbit parameters, *i.e.* the azimuth β, depending on the orbit inclination and latitude of the area of interest, and the inclination to the horizontal θ of the LOS depending on the considered satellite and on the pass being descending or ascending;
- displacement parameters, *i.e.* the azimuth α of displacements, estimated from inclinometer data of the closest monitored vertical, and the inclination to the horizontal ν of displacements, estimated equal to 10° for the studied case.

The inclinometer data of *Costa della Gaveta* earthflow allow highlighting the importance of an accurate estimation of displacement direction, when the component along the LOS represents a small fraction of the total displacement. Figure 6a compares the direction of displacements estimated directly

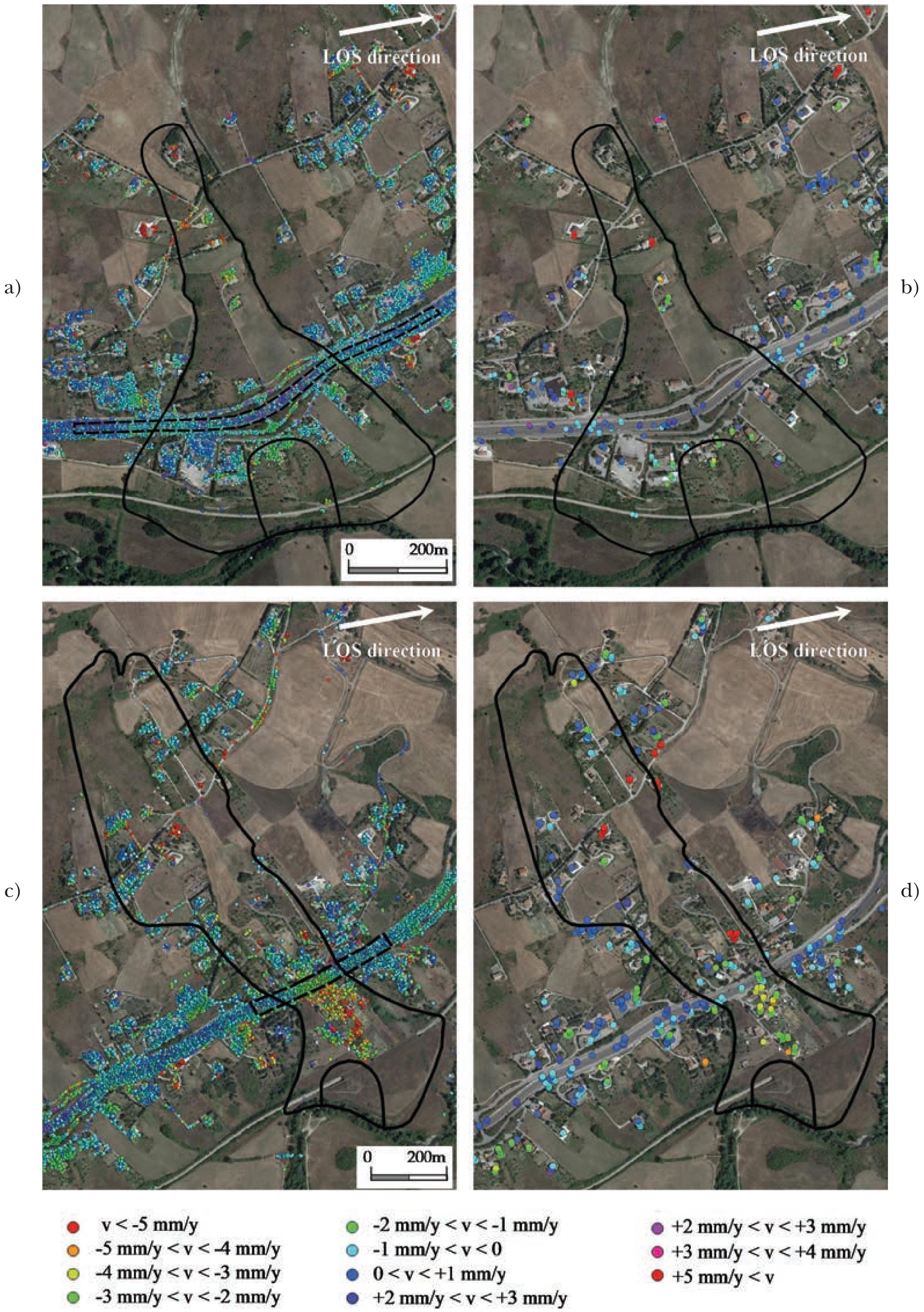

Fig. 4 – Average LOS displacement rates of permanent scatterers for *Costa della Gaveta* earthflow – CSK a) and ENVISAT b) data, and *Varco d'Izzo* earthflow – CSK c) and ENVISAT d) data. Negative values correspond to departure from the sensor along the LOS.

Fig. 4 – Velocità medie lungo la LOS degli scatteratori permanenti per la colata di Costa della Gaveta – dati CSK a) e ENVISAT b), e della colata di Varco d'Izzo – dati CSK c) e ENVISAT d). I valori negativi corrispondono a un allontanamento dal sensore lungo la LOS.

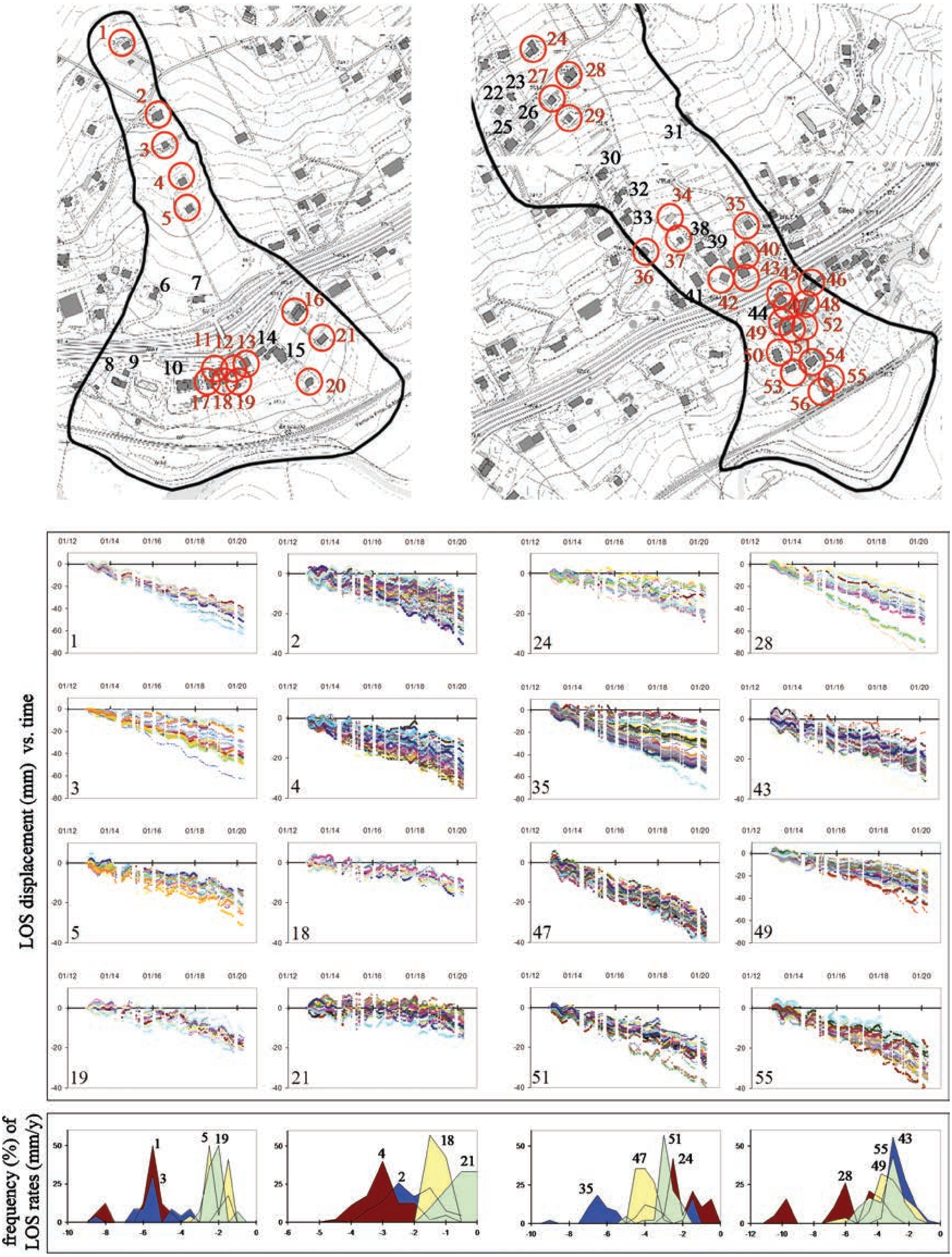

Fig. 5 – CSK data: time series of LOS displacements and statistical distribution of LOS displacement rates for a number of representative displacing targets.

Fig. 5 – Dati CSK: serie temporali degli spostamenti e distribuzione statistica delle velocità lungo la LOS per alcuni punti d'osservazione rappresentativi in movimento.

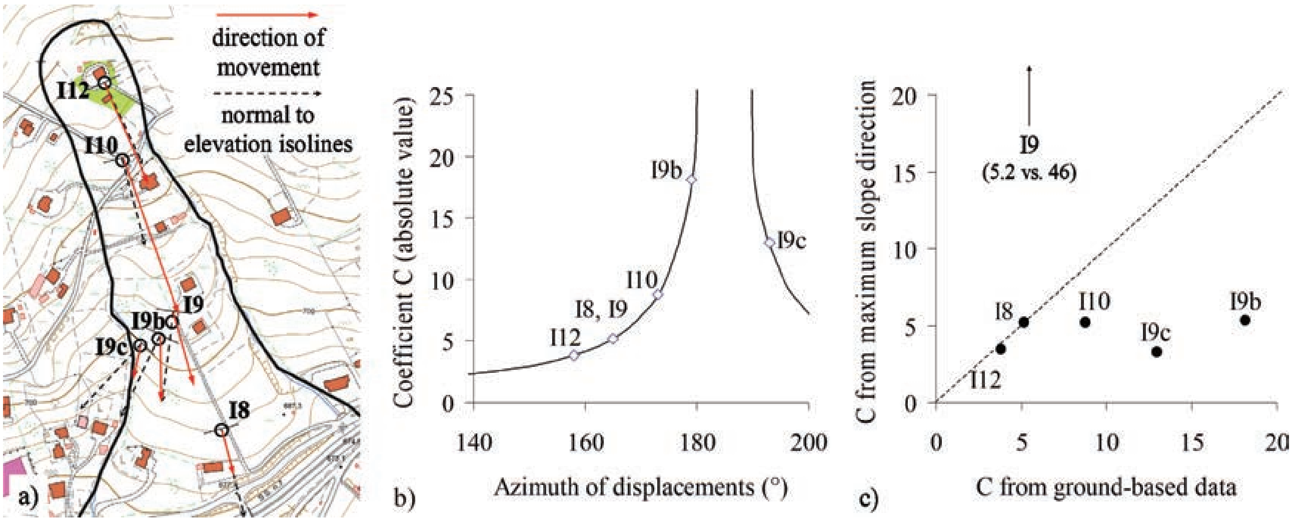

Fig. 6 – Costa della Gaveta earthflow – comparison of the directions of movement and local maximum slope a); coefficient C against azimuth of movement b); comparison between the C values obtained considering either the direction of movement or the direction of maximum slope c).

Fig. 6 – Colata di Costa della Gaveta – confronto tra le direzioni di spostamento e di massima pendenza locale a); coefficiente C in funzione dell'azimut di spostamento b); confronto tra i valori del coefficiente C ottenuti considerando la direzione di spostamento oppure di massima pendenza c).

from inclinometer data to the direction of the local maximum slope of the ground surface. It is worth recalling that, in the literature, the assumption of displacements in the maximum slope direction is quite frequent, especially at the small and medium scale (*e.g.* CALVELLO *et al.*, 2017). In the present study, the large number of available inclinometers allows estimating the error that would be committed by making such assumption. In some cases, the difference in the coefficient *C*, defined as the ratio of horizontal displacements to LOS displacements, is negligible. In other cases, the azimuth difference is significant and, due to the visibility along the LOS of only a small component of the total displacement, the error that would be committed on *C* is noticeable (Figs. 6b-c). This highlights the importance of the ground-based information to properly infer displacements from DInSAR data. Otherwise, the LOS component map might give a strongly distorted picture of the actual landslide kinematics.

To analyze the possible reasons for the variability of displacement time series relative to a single building, figure 7 considers building n. 2 in the main track of *Costa della Gaveta* earthflow. The closest inclinometer, *i.e.* I10, indicates an azimuth of displacements equal to 173°N. The threshold on tomographic coherence was set equal to 0.6, thus selecting only a subset of measurement points showing a higher matching of SAR data with the expected phase model related to elevation and velocity, as explained in Section 4. The resulting displacement rates along the LOS vary approximately from 1 mm/year to 4 mm/year. An approximately linear variation is observed depending on both longitude and latitude, suggesting either a deformation of the building in the horizontal plane (as, *e.g.*, in INFANTE *et al.*, 2019) or a rotation of the building around a horizontal axis. Both phenomena could be actually occurring on site and contributing to the observed data. Considering the slopes of the regression lines of figures 7a-b, the variation seems to be mainly associated to the coordinate X* reported in figure 7d, and negligible orthogonally to X*. If we assume that all the points of the building are moving in the same direction (hypothesis "1", α = 173°N, ν = 10°), then the horizontal displacement rate v_H ranges from 1 cm/year to 3 cm/year (Fig. 7e) and the building is subject to a horizontal deformation rate of 0.08%/year. Conversely, by assuming (hypothesis "2") that the displacements are the results of a rigid translation (with α = 173°N, ν = 10°) plus a rotation around a horizontal axis, then such axis is orthogonal to X* and the rotation, causing a relative heave for the points such as P and settlement for points such as Q, is in order of 0.1 mm/m per year. In figure 7f, the horizontal component of total displacement rates is plotted as a function of X* as resulting from the two hypotheses. Similar results were obtained for other buildings of the slope. For the sake of simplicity, and also due to the unavailability of direct monitoring data relative to the buildings, the average value of v_H deriving from hypothesis "1" will be considered representative (along with standard deviation values). This is very close to assuming hypothesis "2" which, as can be observed in figure 7f, provides v_H values close to the average v_H deriving from hypothesis "1".

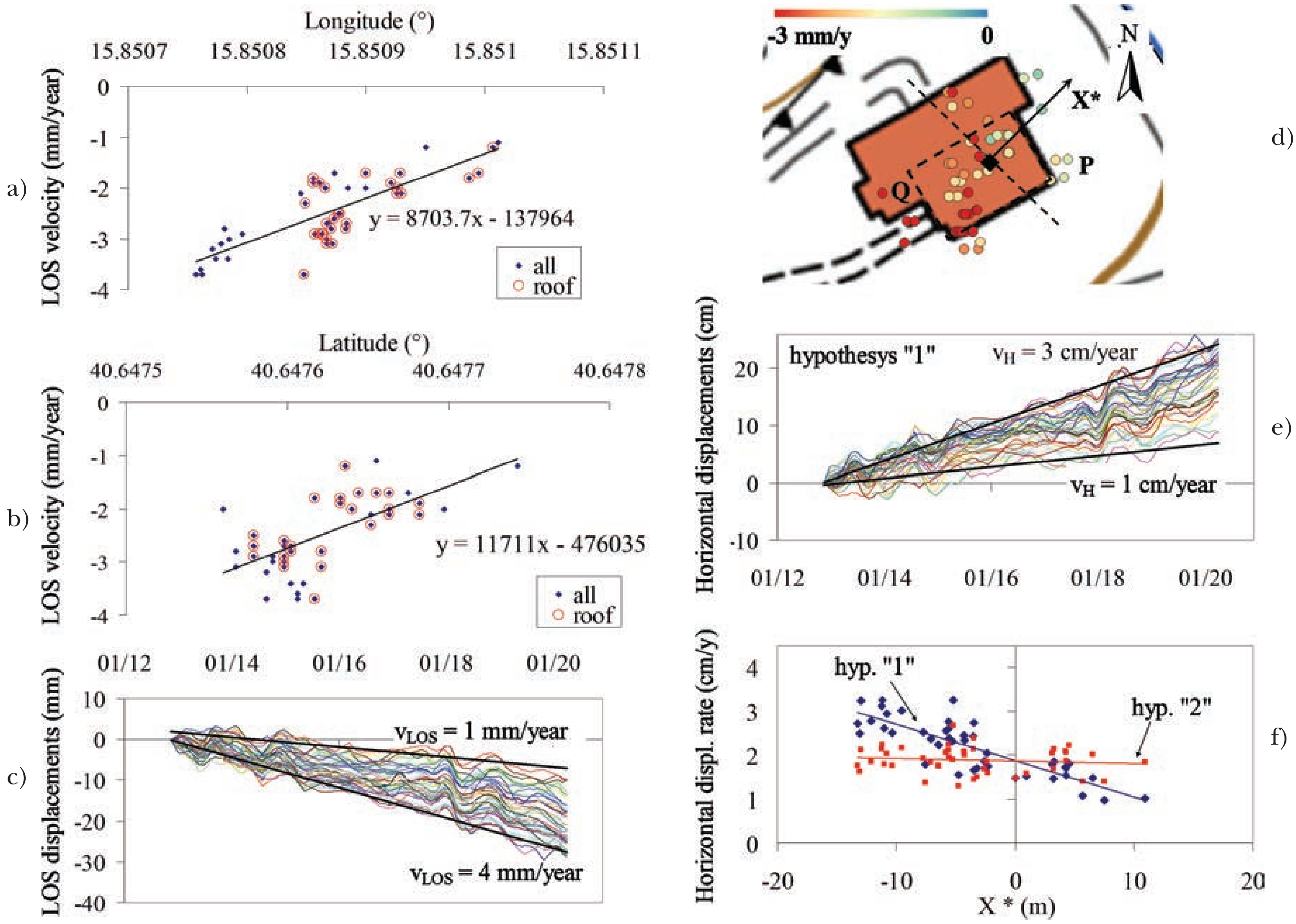

Fig. 7 – CSK data elaboration for building n. 2 of *Costa della Gaveta* earthflow: LOS velocity against longitude a) and latitude b); LOS displacements against time c); LOS velocity map with indication of coordinate X*, whose origin is shown by a black square, and rotation axis (dashed line) d); horizontal displacements against time, calculated under hypothesis "1" e); horizontal displacement rates against X*, calculated under hypotheses "1" (*i.e.* all points are considered to move in the same direction) and "2" (*i.e.*, a rotational effect is contemplated) f).

Fig. 7 – Elaborazione dei dati CSK dell'edificio n. 2 ubicato nella colata di Costa della Gaveta: velocità lungo la LOS in funzione della longitudine a) e della latitudine b); spostamenti lungo la LOS in funzione del tempo c); mappa delle velocità lungo la LOS con indicazione dell'asse X, la cui origine è rappresentata da un quadrato nero, e dell'asse di rotazione (linea tratteggiata) d); spostamenti orizzontali in funzione del tempo, calcolati nell'ipotesi "1" e); spostamenti orizzontali in funzione della coordinata X*, calcolati nell'ipotesi "1" (assumendo che tutti i punti si muovano nella stessa direzione) e "2" (considerando un effetto rotazionale) f).*

In the areas where ground-based and GPS data are available for a long time span, it is worth comparing them to DInSAR data. Figure 8 reports such comparison for two representative locations. DInSAR data are consistent with those of inclinometers I9, I9b and I9bis in *Costa della Gaveta* earthflow (Fig. 8b) and with those of GPS permanent station F2 in *Varco d'Izzo* earthflow (Fig. 8c). Further evidence of the good agreement between remote sensing and ground-based data is provided in the following sections. Such agreement encourages the use of DInSAR data to enhance the description of the displacement evolution in time and its distribution in space.

The National Road crosses both the investigated earthflows. In the case of *Varco d'Izzo*, whose displacement rates are higher than those of *Costa della Gaveta*, the footprint of landslide displacements along the road is quite evident from DInSAR data (as shown by the LOS velocity map of Fig. 4c). This is analyzed in detail in figure 9. For comparison, LOS average displacement rates are reported in figure 9b for the road sector that crosses *Costa della Gaveta* earthflow (dashed area in Fig. 4a). The figure allows to appreciate the movement of a stretch of road approximately 150 m long, internal to the landslide boundaries detected from geological observations. Displacements against time are also reported in figure 9c for the middle point of such stretch, which underwent 15 mm LOS displacements in 7 years. If we assume that displacements have the direction of

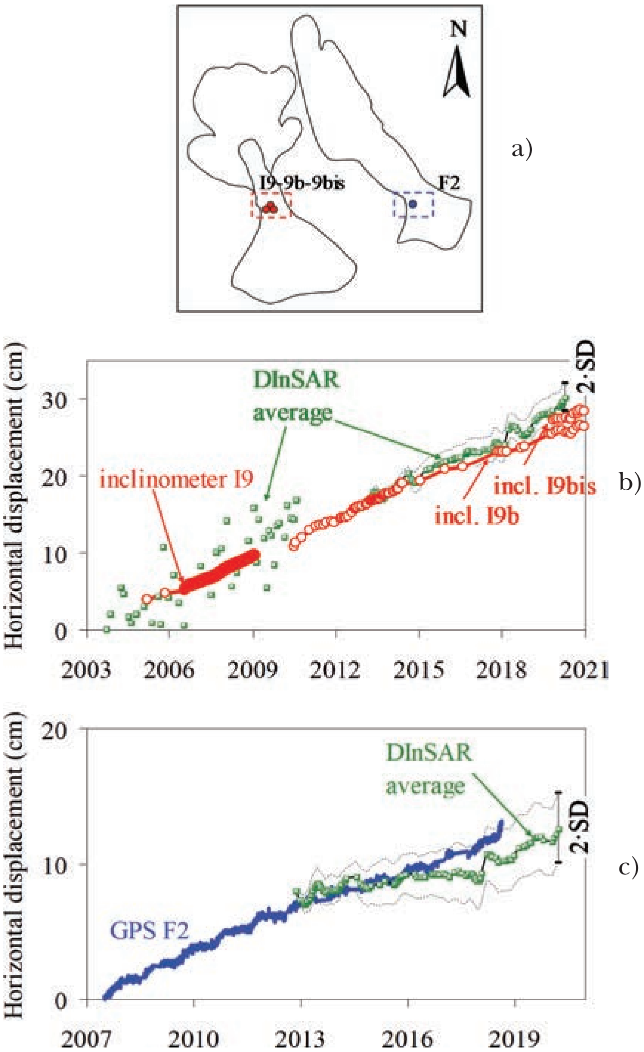

Fig. 8 – Comparison of displacements obtained from inclinometer, GPS, and DInSAR data represented by average values and standard deviation (SD): position of inclinometers and GPS station (a); time series relative to *Costa della Gaveta* (b) and *Varco d'Izzo* (c) earthflows. GPS F2 data from Calcaterra *et al.* [2012] and Vassallo *et al.* [2020].

Fig. 8 – Confronto tra gli spostamenti ottenuti dai dati inclinometrici, GPS e DInSAR, con questi ultimi rappresentati in termini di valori medi e deviazione standard (SD): posizione degli inclinometri e della stazione GPS (a); serie temporali relative alle colate di Costa della Gaveta (b) e Varco d'Izzo (c). I dati del GPS F2 sono riportati da Calcaterra et al. *[2012] e Vassallo* et al. *[2020].*

the nearby inclinometers, this corresponds to an average rate of movement of 1 cm/year.

Figure 10 shows the data relative to the zone of *Varco d'Izzo* earthflow situated between the National Road and the railway. A threshold for coherence equal to 0.6 was set, thus selecting approximately half of the available 1500 points, with their displacement time series. Displacements along the LOS are plotted along axis Y*, corresponding to the landslide longitudinal axis, for approximately two year intervals. A statistical elaboration of the data was carried out by drawing the parabolas interpolating the 90th percentile of the displacements detected on every 20 m along Y*. Figure 10c also reports the time series of LOS displacements for three points of the parabolas (namely, the white, grey and black dots of Fig. 10b). Every parabola has its maximum halfway between the National Road and the railway, both reinforced by pile walls that hinder landslide displacements. However, such interpolating curves might give a distorted image of the landslide dynamics for a number of reasons. First of all, satellite data reflect superficial displacements, whose relationship with deep displacements might not be uniform in the analyzed area. In particular, the contribution of the shallowest soil horizons to total displacements might be more significant in the middle, and less significant close the pile walls of the road and the railway. Second, there is a probable change of displacement direction from upslope to downslope, due to the presence of a local landslide at the toe caused by river erosion (Fig. 1b; Vassallo *et al.*, 2020). Specifically, in the lower half of the considered zone, the reduction of LOS velocities in the downslope direction might be partly due to an increase of azimuth rather than an actual decrease of total displacement rates.

6. Temporal and spatial extension of ground-based data by means of DInSAR data

If the Envisat data are also considered, a time span of almost 20 years can be analyzed. Figure 11 reports the examples of DInSAR data close to inclinometers I12 of *Costa della Gaveta* earthflow, I3 and I5 of *Varco d'Izzo* earthflow. The data of the different satellite systems can be considered in substantial continuity, showing practically the same average displacement rates. Satellite data allow to fill the gaps of information present in ground-based data or to extend them forward in time.

Figure 12 compares, for the accumulation of *Varco d'Izzo* earthflow, the satellite data – including ERS data in the period 1992-2000 – to the inclinometer data since 1990. In particular, figure 12b refers to the zone closer to the National Road, while figure 12c refers to the zone that is halfway between the National Road and the railway, *i.e.* close, respectively, to buildings n. 48 and n. 54 of figure 5. Inclinometers installed before 2005, such as B25, FSC, S1f and B24 were monitored for quite a short period. Their data were mostly useful for the evaluation of slip surfaces depth and, thus, for the reconstruction of the 3D landslide geometry [Di Maio *et al.*, 2012; Vassallo *et al.*, 2019]. Nevertheless, their superficial displacement time series give further useful information if

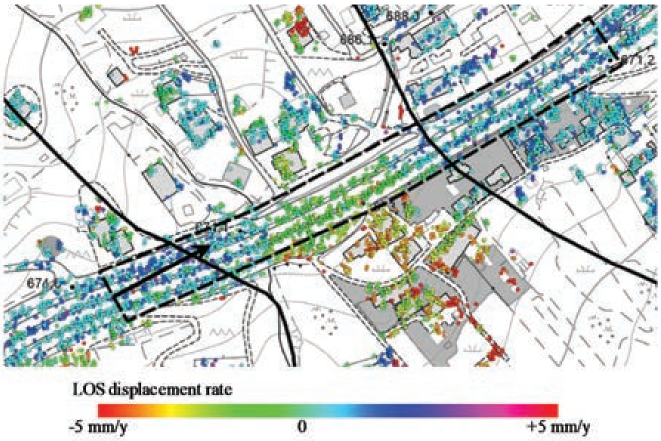

a)

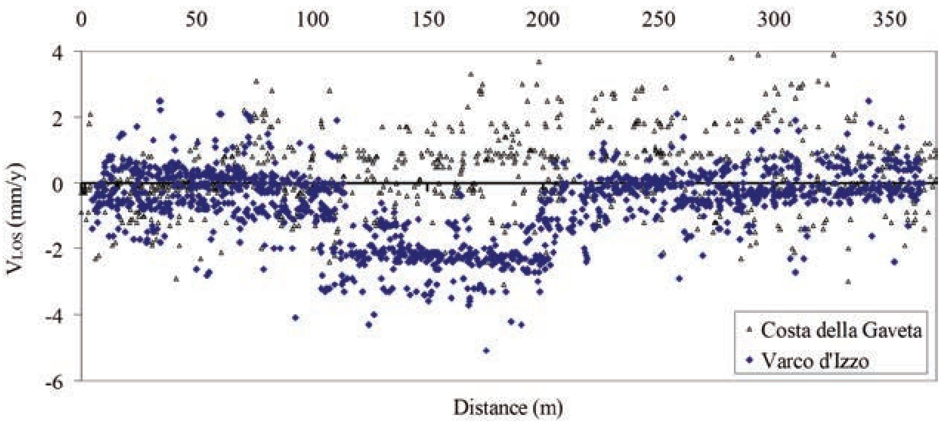

b)

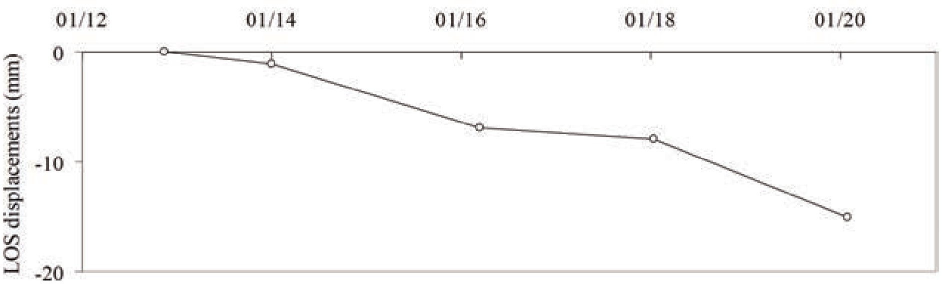

c)

Fig. 9 – Analysis of CSK data relative to the National Road: distribution of LOS average displacement rates in the area of *Varco d'Izzo* earthflow a); LOS average displacement rates against distance for *Costa della Gaveta* and *Varco d'Izzo* erthflows b); LOS displacements against time for the stretch of road crossing the accumulation of *Varco d'Izzo* erthflow c).

Fig. 9 – Analisi dei dati CSK relativi alla Strada Statale Basentana: distribuzione delle velocità medie lungo la LOS nella zona di Varco d'Izzo a); velocità medie lungo la LOS in funzione della distanza per le colate di Costa della Gaveta e Varco d'Izzo b); spostamenti lungo la LOS in funzione del tempo per il tratto di Statale che attraversa l'accumulo della colata di Varco d'Izzo c).

analyzed together with the satellite data. Apparently, higher displacement rates occurred in the period 1992-2000, *i.e.* until 8 years after the construction of the pile walls protecting the railway. From 2000 on, lower displacement rates were recorded, with yearly values fundamentally constant until nowadays.

The field of the average rates of superficial displacements, reported in figures 13a-b, was obtained by combining all the available information deriving from inclinometer, GPS, and DInSAR data, and aims at giving a complete picture of the main kinematic features of the investigated landslides. It confirms that in *Costa della Gaveta* earthflow the displacement rates sensibly decrease from upslope to downslope along the landslide body. The movement seems continuous along the landslide longitudinal axis. In the source area, close to the landslide head, the satellite data indicate significant displacements that represent a warning for a possible reactivation and thus highlight the need for further investigation. The accumulation shows rates an order of magnitude lower than the main track. The extremely slow movements of this sector have exhibited a practically steady state pattern in the last 16

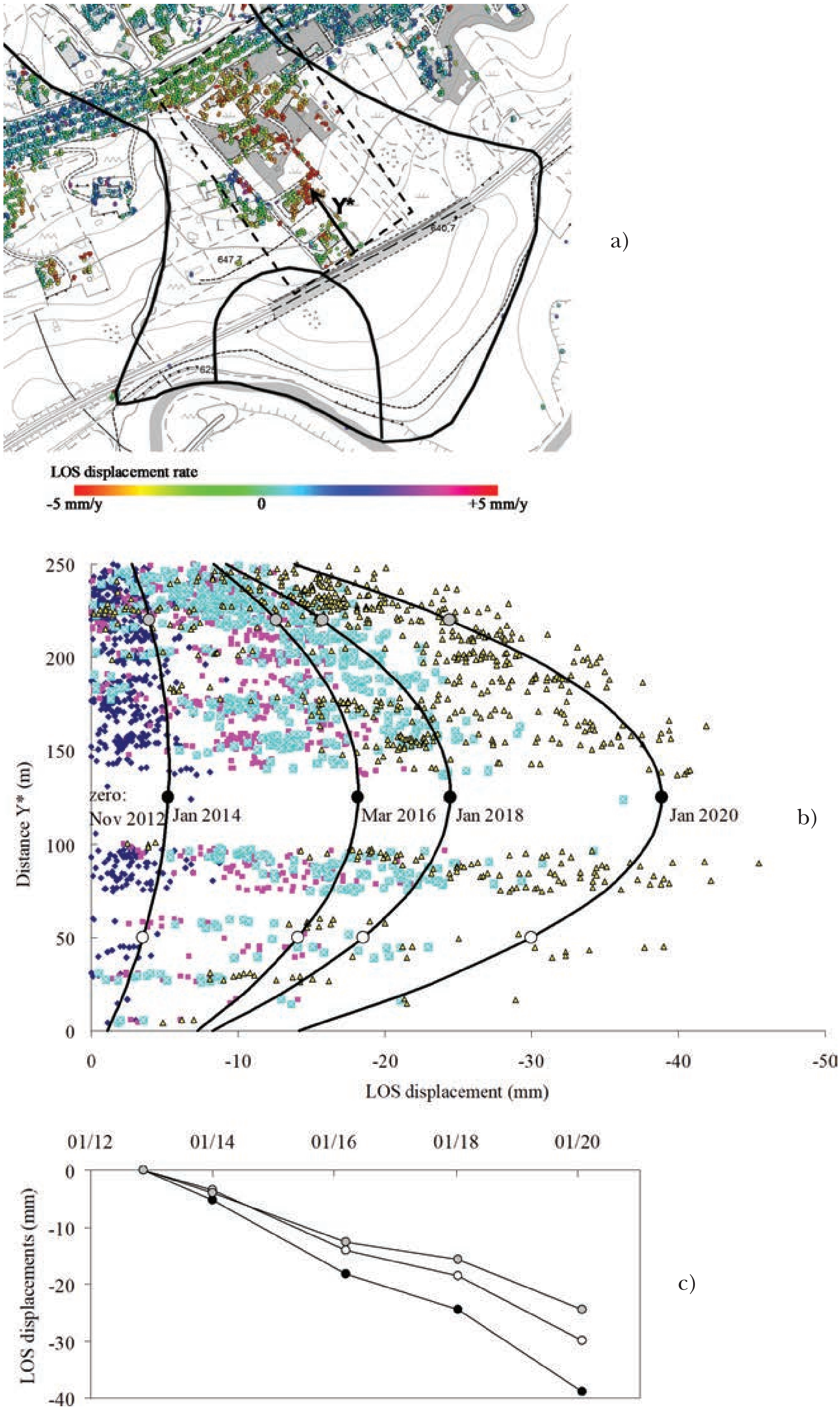

Fig. 10 – Analysis of CSK data relative to the accumulation of *Varco d'Izzo* earthflow: distribution of LOS average displacement rates a); LOS displacements against distance on different dates with parabolic interpretation b); LOS displacements against time of three points of the parabolas c).

Fig. 10 – Analisi dei dati CSK relativi all'accumulo della colata di Varco d'Izzo: distribuzione delle velocità medie lungo la LOS a); spostamenti lungo la LOS in funzione della distanza per varie date, con interpretazione parabolica b); spostamenti lungo la LOS in funzione del tempo per tre punti delle parabole c).

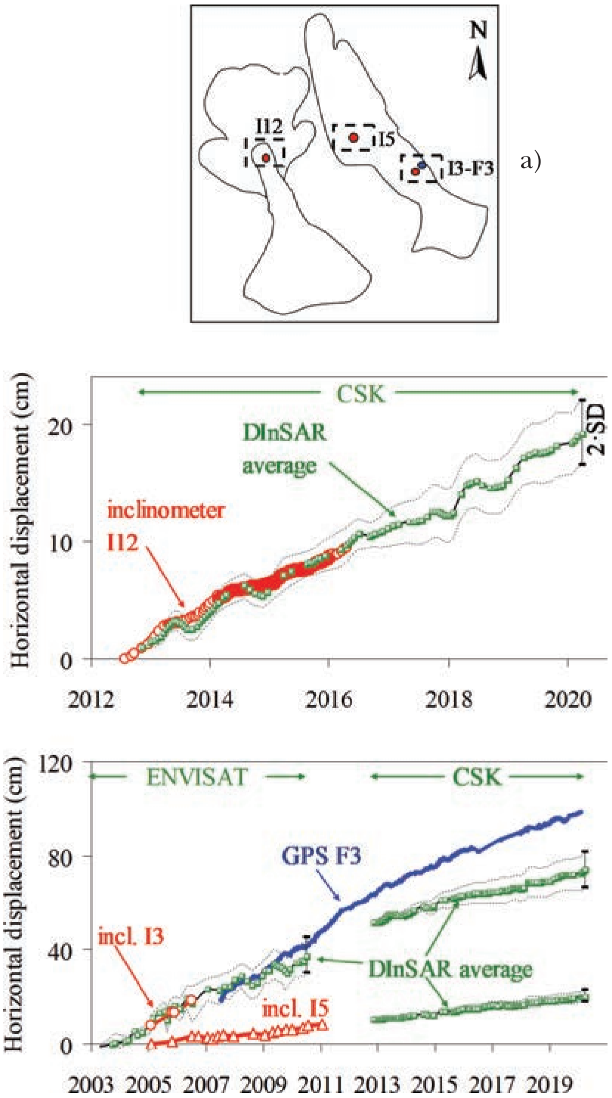

Fig. 11 – Displacements against time from inclinometer, GPS and DInSAR data in the period 2003-2020: position of inclinometers and GPS station a); time series relative to *Costa della Gaveta* b) and *Varco d'Izzo* c) earthflows. GPS F3 data from CALCATERRA *et al.* [2012] and VASSALLO *et al.* [2020].

Fig. 11 – Spostamenti in funzione del tempo stimati da dati inclinometrici, GPS e DInSAR nel periodo 2003-2020: posizione degli inclinometri e della stazione GPS a); serie temporali relative alle colate di Costa della Gaveta b) e Varco d'Izzo c). I dati del GPS F3 sono riportati da CALCATERRA et al. *[2012] e VASSALLO* et al. *[2020].*

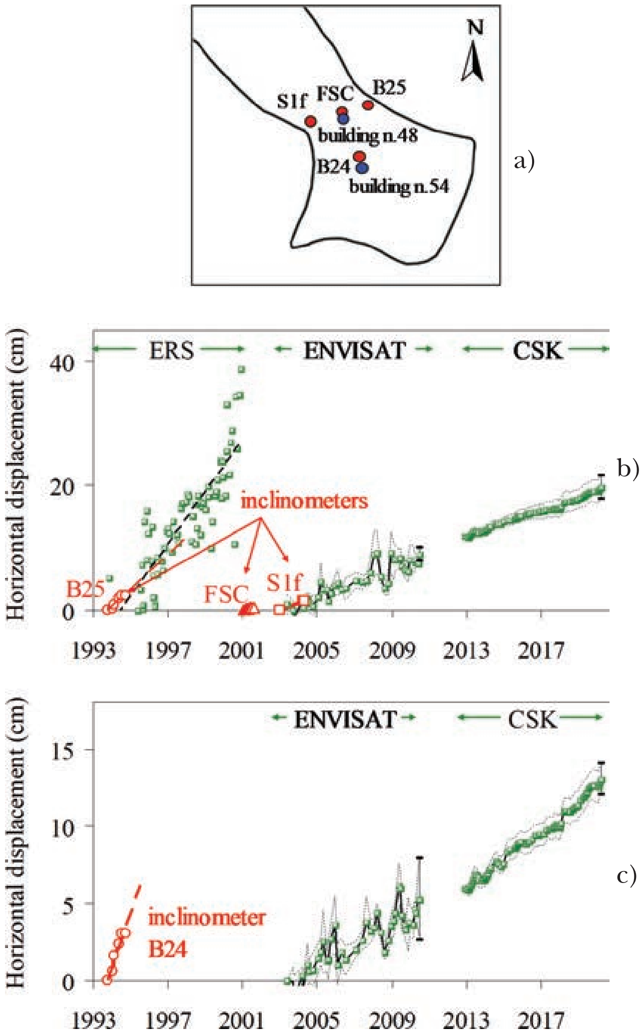

Fig. 12 – Horizontal displacements of inclinometers and nearby buildings n. 48 and 54 (DInSAR data) in the period 1993-2020: position of inclinometers and buildings a); time series relative to the upper b) and middle c) zones of the accumulation of *Varco d'Izzo* earthflow.

Fig. 12 – Spostamenti orizzontali derivanti dalle misure inclinometriche e dai dati DInSAR degli edifici n. 48 and 54 nel periodo 1993-2020: posizione degli inclinometri e degli edifici a); serie temporali relative alla zona superiore b) e centrale c) dell'accumulo della colata di Varco d'Izzo.

years, as shown by figures 3a-b. The central part of the accumulation undergoes slightly higher rates, probably linked to the presence of a local slide related to the river erosion at the toe [VASSALLO *et al.*, 2012]. More complete indications will be obtained after further monitoring of deep displacements. The Basento river is characterized by pronounced bends, reasonably related to the historical landslide activity affecting both of the banks. Some of the current movements of the slope opposite to *Costa della Gaveta* are detected by DInSAR data, as shown in figure 13b.

A number of buildings located between the accumulations of *Costa della Gaveta* and *Varco d'Izzo* earthflows also show non negligible displacement rates related to shallow instabilities.

Varco d'Izzo earthflow is characterized by a more heterogeneous and less continuous displacement rate distribution. An upper zone, close to inclinometer I5, shows rates in the order of 1 cm/y. A central zone close to inclinometer I4 showed negligible displacements over the monitoring period. This zone seems to extend to some buildings downslope,

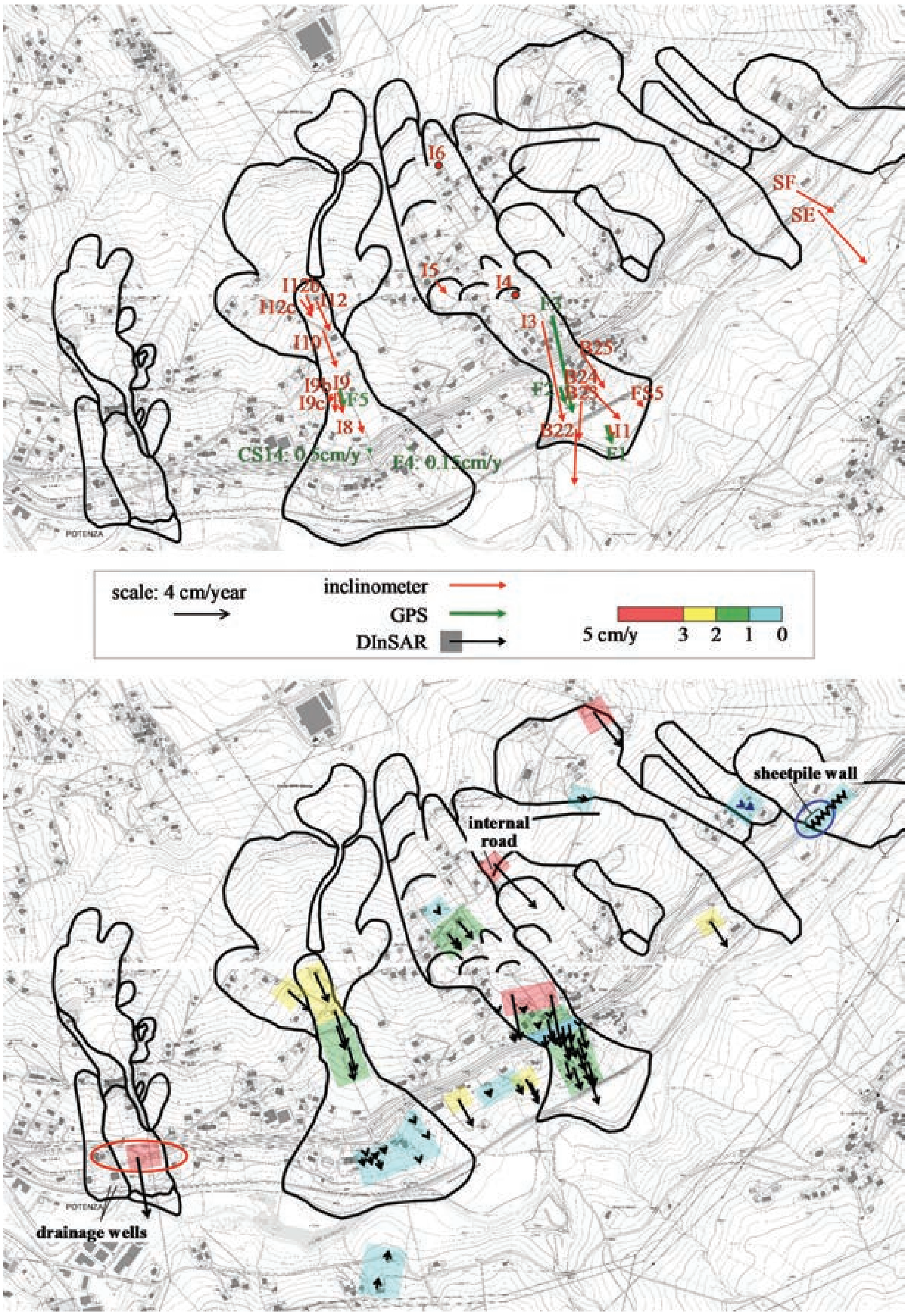

Fig. 13 – Displacement rate maps of the study area from inclinometer and GPS a) and DInSAR b) data.
Fig. 13 – Mappe di velocità dell'area di studio ricavate dai dati inclinometrici e GPS a) e DInSAR b).

east of inclinometer I3 and GPS F3. The lower zone between I3 and the river, which is also the most urbanized one, shows displacement rates which stayed fundamentally constant in the last 15 years and range between 7 cm/y and 1 cm/y. Both values and directions of displacements measured by inclinometers before 2000 suggest a different and more intense phase of activity at that time.

East of *Varco d'Izzo* earthflow, a number of targets with significant velocities can be identified from DInSAR data, mainly located along the landslide scarps.

Figures 14 and 15 depict the effects of two remedial measures that were realized on the investigated slope by different public entities. Their location is encircled in figure 13b.

In the western sector of the slope, two deep drainage wells were constructed between 1988 and 1994 to reduce the velocities of a large landslide involving some buildings and the highway junction (Fig. 14a). Even if DInSAR data do not go back to before the construction of the wells, they give useful indication about the landslide activity of the last 17 years. The rates of displacement series reported in

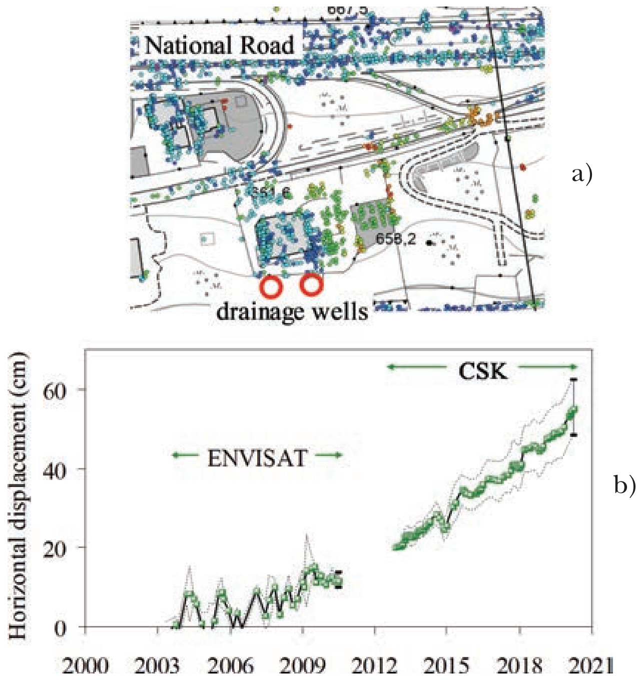

Fig. 14 – CSK LOS diplacement rate map a) and horizontal displacement time series b) in the proximity of drainage wells, constructed in the period between 1988 and 1994.
Fig. 14 – Mappa degli spostamenti CSK lungo la LOS a) e serie temporale degli spostamenti orizzontali b) in prossimità dei pozzi drenanti, realizzati tra il 1988 e il 1994.

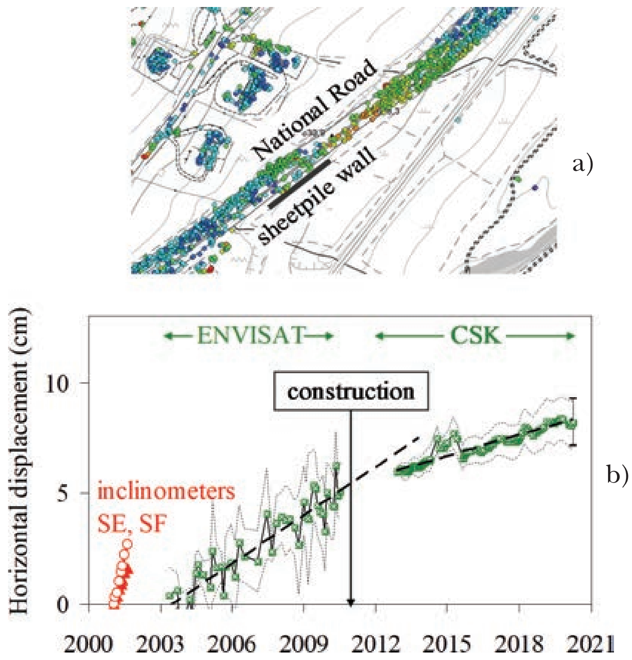

Fig. 15 – CSK LOS diplacement rate map a) and horizontal displacement time series b) in the proximity of a pile wall protecting the National Road.
Fig. 15 – Mappa degli spostamenti CSK lungo la LOS a) e serie temporale degli spostamenti orizzontali b)in prossimità della paratia costruita a protezione della Strada Statale Basentana.

figure 14b appear almost constant (or even slightly increasing if we compare Envisat to CSK data) and are in the order of 3 cm/year, notwithstanding the presence of the drainage system.

In the eastern sector of the slope, because of the frequent damage to the National Road, a 75 m-long pile wall was constructed in 2011 by large diameter contiguous bored concrete piles (Fig. 15a). The previous landslide activity in this zone is also attested by the data of 2002 of inclinometers SE and SF (displacement rate vectors reported in Fig. 13a). DInSAR data allow appreciating, after the wall construction, a significant displacement rate decrease, to approximately half the previous value, *i.e.* less than 0.5 cm/year (Fig. 15b).

7. Conclusions

This paper showed the results of a long-term ground-based monitoring of the slow movements of two earthflows occurring in the structurally complex Variegated Clays formation. With the aim of enlarging the investigated areas and taking advantage of the availability of long data series dating back to 1993, the possibility of using ERS, Envisat and COSMO-SkyMed satellite data has been investigated.

The mostly N-S orientation of displacements makes monitoring with the satellite interferometry methodology not immediate. To minimize such problem, the satellite data relative to areas where the displacements and their directions are clearly determined by inclinometers and GPS were analysed in detail. The knowledge of displacement directions by ground-based measurements made it possible to convert the displacement component along the LOS into total displacement. Images acquired by the COSMO-SkyMed satellite system, supplemented by ERS and Envisat data, were thus used to reconstruct rather continuous displacement series which: i) filled the gaps of ground-based measurement series, ii) allowed to confidently exploit displacement field information in areas wider than those investigated by ground sensors.

The results obtained by the different ground and satellite sensors allowed the evaluation of the time trend of the displacement fields over a 30 year time interval, and gave an indication on the effectiveness of the remedial measures constructed in the area as well as on the necessity of further investigations in some zones.

Satellite data also allowed for the identification of the most active areas within the landslides and thus provided extensive information for the detection of possible triggers. Besides the current information, future satellite data, whose physical meaning has been ascertained, will bring on the monitoring of the considered areas when, in the future, the inclinometers will go out of use.

Acknowledgments

The Authors would like to thank the Italian Space Agency (ASI) for providing the Cosmo-SkyMed data set through the ASI Open Call for Science Project ID-763. This research has been supported by MIUR PON R&I 2014-2020 Program (project MITIGO, ARS01_00964).

References

Antronico L., Borrelli L., Coscarelli R., Gullà G. (2015) – *Time evolution of landslide damages to buildings: The case study of Lungro (Calabria, Southern Italy).* Bulletin of Engineering Geology and the Environment, 74, pp. 47-59.

Borrelli L., Nicodemo G., Ferlisi S., Peduto D., Di Nocera S., Gullà G. (2018) – *Geology, slow-moving landslides, and damages to buildings in the Verbicaro area (North-western Calabria region, Southern Italy).* Journal of Maps, 14, n. 2, pp. 32-44.

Bovenga F., Pasquariello G., Pellicani R., Refice A., Spilotro G. (2017) – *Landslide monitoring for risk mitigation by using corner reflector and satellite SAR interferometry: the large landslide of Carlantino (Italy).* Catena, 151, pp. 49-62.

Bru G., González P.J, Mateos R.M., Roldán F.J., Herrera G., Béjar-Pizarro M., Fernández J. (2017) – *A-DInSAR Monitoring of Landslide and Subsidence Activity: A Case of Urban Damage in Arcos de la Frontera, Spain.* Remote Sensing, 9, n. 8, p. 787.

Calcaterra S., Di Maio C., Gambino P., Vallario M., Vassallo R. (2012) – *Surface displacements of two landslides evaluated by GPS and inclinometer systems: a case study in Southern Apennines, Italy.* Natural Hazards, 61, pp. 257-266.

Calò F., Ardizzone F., Castaldo R., Lollino. P., Tizzani P., Guzzetti F., Lanari R., Angeli M.G., Pontoni F., Manunta M. (2014) – *Enhanced landslide investigations through advanced DInSAR techniques: the Ivancich case study, Assisi, Italy.* Remote Sensing of Environment, 142, pp. 69-82.

Calvello M., Peduto D., Arena L. (2017) – *Combined use of statistical and DInSAR data analyses to define the state of activity of slow-moving landslides.* Landslides, 14, pp. 473-489.

Cascini L., Fornaro G., Peduto D. (2010) – *Advanced low-and full-resolution DInSAR map generation for slow-moving landslide analysis at different scales.* Engineering Geology, 112, n. 1-4, pp. 29-42.

Cascini L., Peduto D., Pisciotta G., Arena L., Ferlisi S., Fornaro G. (2013) – *The combination of DInSAR and facility damage data for the updating of slow-moving landslide inventory maps at medium scale.* Natural Hazards and Earth System Sciences, 13, pp. 1527-1549.

Cascini L., Calvello M., Grimaldi G.M. (2014) – *Displacement trends of slow-moving landslides: Classification and forecasting.* Journal of Mountain Science, 11, n. 3, pp. 592-606.

Colesanti C., Wasowski J. (2006) – *Investigating landslides with space-borne Synthetic Aperture Radar (SAR) interferometry.* Engineering Geology, 88, nn. 3-4, pp. 174-199.

Confuorto P., Di Martire D., Infante D., Novellino A., Papa R., Calcaterra D., Ramondini M. (2019) – *Monitoring of remedial works performance on landslide-affected areas through ground- and satellite-based techniques.* Catena, 178, pp. 77-89.

Corominas J., van Westen C., Frattini P., Cascini L., Malet J.P., Fotopoulou S., Catani F., Van Den Eeckhaut M., Mavrouli O., Agliardi F., Pitilakis K., Winter M.G., Pastor M., Ferlisi S., Tofani V., Hervàs J., Smith J.T. (2014) – *Recommendations for the quantitative analysis of landslide risk.* Bulletin of Engineering Geology and the Environment, 73, n. 2, pp. 209-263.

Costantini M., Ferretti A., Minati F., Falco S., Trillo F., Colombo D., Novali F., Malvarosa F., Mammone C., Vecchioli F., Rucci A, Fumagalli A., Allievi J., Ciminelli M.G., Costabile S. (2017) – *Analysis of surface deformations over the whole Italian territory by interferometric processing of ERS, Envisat and COSMO-SkyMed radar data.* Remote Sensing of Environment, 202, pp. 250-275.

Crosta G., Agliardi F., Rivolta C., Alberti S., Dei C.L. (2017) – *Long-term evolution and early warning strategies for complex rockslides by real-time monitoring.* Landslides, 14, n. 5, pp. 1615-1632.

De Maio A., Fornaro G., Pauciullo A. (2009) – *Detection of single scatterers in multidimensional SAR imaging.* IEEE Trans. EEE Transactions on Geoscience and Remote Sensing, 47, n. 7, pp. 2284-2997.

Di Maio C., Vassallo R., Vallario M., Pascale S., Sdao F. (2010) – *Structure and kinematics of a landslide in a complex clayey formation of the Italian Southern Apennines.* Engineering Geology, 116, pp. 311-322.

Di Maio C., Vallario M., Vassallo R., Bianca M. (2012) – *Displacements of a large landslide in structurally complex clays.* Proc. 11th Int. Symposium on Landslides and Engineered Slopes, Banff, Canada, CRC Press, Taylor & Francis Group, 1, pp. 607-613.

Di Maio C., Vassallo R., Vallario M. (2013) – *Plastic and viscous displacements of a deep and very slow landslide in stiff clay formation.* Engineering Geology, 162, pp. 53-66.

Di Maio C., Scaringi G., Vassallo R. (2015) – *Residual strength and creep behaviour on the slip surface of specimens of a landslide in marine origin clay shales: influ-*

ence of pore fluid composition. Landslides, 12, n. 4, pp. 657-667.

Di Maio C., Vassallo R., Scaringi G., De Rosa J., Pontolillo D.M., Grimaldi G.M. (2017) – *Monitoring and analysis of an earthflow in tectonized clay shales and study of a remedial intervention by KCl wells.* Rivista Italiana di Geotecnica, 51, pp. 48-63.

Di Maio C., Fornaro G., Gioia D., Reale D., Schiattarella M., Vassallo R. (2018) – *In situ and satellite long-term monitoring of the Latronico landslide, Italy: displacement evolution, damage to buildings, and effectiveness of remedial works.* Engineering Geology, 245, pp. 218-235.

Di Maio C., De Rosa J., Vassallo R., Coviello R., Macchia G. (2020) – *Hydraulic conductivity and pore water pressures in a clayey earthflow: Experimental data.* Geosciences, 10, p. 102.

Di Maio C., De Rosa J., Vassallo R. (2021) – *Pore water pressures and hydraulic conductivity in the slip zone of a clayey earthflow: Experimentation and modelling.* Engineering Geology, 292, 106263, https://doi.org/10.1016/j.enggeo.2021.106263

Ferlisi S., Gullà G., Nicodemo G., Peduto D. (2019) – *A multi-scale methodological approach for slow-moving landslide risk mitigation in urban areas, Southern Italy.* Euro-Mediterranean Journal for Environmental Integration, 4, n. 20, 15 pp.

Ferlisi S., Marchese A., Peduto D. (2021) – *Quantitative analysis of the risk to road networks exposed to slow-moving landslides: a case study in the Campania region (Southern Italy).* Landslides, 18, pp. 303-319.

Ferrigno F., Gigli G., Fanti R., Casagli N. (2015) – *GB-InSAR monitoring and observational method for landslide emergency management: the Montaguto earthflow (AV, Italy).* Natural Hazards and Earth System Sciences Discussions, 3, pp. 7247-7273.

Fornaro G., Pauciullo A., Serafino F. (2009) – *Deformation monitoring over large areas with multipass differential SAR interferometry: a new approach based on the use of spatial differences.* International Journal of Remote Sensing, 30, n. 6, pp. 1455-1478.

Fornaro G., Pauciullo A., Reale D., Verde S. (2014) – *Multilook SAR tomography for 3-D reconstruction and monitoring of single structures applied to COSMO-SkyMed data.* IEEE Journal of Selected Topics in Applied Earth Observations and Remote Sensing, 7, pp. 2776-2785.

Glastonbury J., Fell R. (2008) – *Geotechnical characteristics of large slow, vey slow, and extremely slow landslides.* Canadian Geotechnical Journal, 45, pp. 984-1005.

Guida D., Iaccarino G. (1991) – *Fasi evolutive delle frane tipo colata nell'alta valle del F. Basento (Potenza).* Studi trentini di scienze naturali, Acta Geologica, 68, pp. 127-152.

Handwerger A.L., Roering J.J., Schmidt D.A. (2013) – *Controls on the seasonal deformation of slow-moving landslides.* Earth and Planetary Science Letters, nn. 377-378, pp. 239-247.

Herrera G., Gutiérrez F., García-Davalillo J.C., Guerrero J., Notti D., Galve J.P., Fernández- Merodo J.A., Cooksley G. (2013) – *Multi-sensor advanced DInSAR monitoring of very slow landslides: the Tena Valley case study (Central Spanish Pyrenees).* Remote Sensing of Environment, 128, pp. 31-43.

Hungr O., Leroueil S., Picarelli L. (2014) – *The Varnes classification of landslide types, an update.* Landslides, 11, pp. 67-194.

Infante D., Di Martire D., Confuorto P., Tessitore S., Tòmas R., Calcaterra D., Ramondini M. (2019) – *Assessment of building behavior in slow-moving landslide-affected areas through DInSAR data and structural analysis.* Engineering Structures, 199, art. n. 109638, 16 pp.

Journault J., Macciotta R., Hendry M.T., Charbonneau F., Huntley D., Bobrowsky P.T. (2018) – *Measuring displacements of the Thompson River valley landslides, south of Ashcroft, BC, Canada, using satellite InSAR.* Landslides, 15, n. 4, pp. 621-636.

Kavoura K., Konstantopoulou M., Depountis N, Sabatakakis N. (2020) – *Slow-moving landslides: kinematic analysis and movement evolution modelling.* Environmental Earth Sciences, 79, n. 130, 11 pp.

Mansour M.F., Morgenstern N.I., Martin C.D. (2011) – *Expected damage from displacement of slow-moving slides.* Landslides, 8, n. 1, pp. 117-131.

Minardo A., Picarelli L., Catalano E., Coscetta A., Zeni G., Zhang L., Di Maio C., Vassallo R., Coviello R., Macchia G., Zeni L. (2018) – *Distributed Fiber Optic Sensors for the Monitoring of a Tunnel Crossing a Landslide.* Remote Sensing, 10, 1291.

Nappo N., Peduto D., Mavrouli O., van Westen C.J., Gullà G. (2019) – *Slow-moving landslides interacting with the road network: analysis of damage using ancillary data, in situ surveys and multi-source monitoring data.* Engineering Geology, 260, 105244.

Nikolaeva E., Walter T.R., Shirzaei M., Zschau J. (2013) – *Landslide observation and volume estimation in central Georgia based on L-band InSAR.* Natural Hazards and Earth System Sciences, 14, pp. 675-688.

North M., Farewell T., Hallet S., Bertelle A. (2017) – *Monitoring the response of roads and railways to seasonal soil movement with persistent scatterers interferometry over six UK sites.* Remote Sensing, 9, pp. 1-17.

Noviello C., Verde S., Zamparelli V., Fornaro G., Pauciullo A., Reale D., Nicodemo G., Ferlisi S., Gullà G., Peduto D. (2020) – *Monitoring Buildings at Landslide Risk With SAR: A Methodology Based on the Use of Multipass Interferometric Data.* IEEE Geoscience and Remote Sensing Magazine, 8, n. 1, pp. 91-119.

Peduto D., Cascini L., Arena L., Ferlisi S., Fornaro G., Reale D. (2015) – *A general framework and related procedures for multiscale analyses of DInSAR data in subsiding urban areas.* ISPRS Journal of Photogrammetry and Remote Sensing, 105, pp. 186-210, https://doi.org/10.1016/j.isprsjprs.2015.04.001

Peduto D., Santoro M., Aceto L., Borrelli L., Gullà G. (2020) – *Full integration of geomorphological, geotechnical, A-DInSAR and damage data for detailed geometric-kinematic features of a slow-moving landslide in urban area.* Landslides, 18, pp. 807-825.

Picarelli L. (2007) – *Considerations about the mechanics of slow active landslides in clay.* Progress in Landslide Science, K. Sassa, H. Fukuoka, F. Wang, G. Wang (Eds.), Springer, pp. 27-45.

Picarelli L., Russo C. (2004) – *Mechanics of slow active landslides and interaction with man-made works.* Keynote Lecture, Proc. 9th Int. Symposium on Landslides, Rio de Janeiro, Balkema, 2, pp. 1141-1176.

Picarelli L., Di Maio C. (2010) – *Deterioration processes of hard clays and clay shales.* Geological Society, London, Engineering Geology Special Publications, 23, pp. 15-32.

Picarelli L., Comegna L., Damiano E., Olivares L., Urciuoli G. (2021) – *Hydro-mechanical slope response to weather impact.* Keynote Lecture, Proc. 13th Int. Symposium on Landslides, Cartagena, Colombia, 22-26 February 2021, Online Library of the International Society for Soil Mechanics and Geotechnical Engineering (ISSMGE), 25 pp., https://www.issmge.org/uploads/publications/105/106/ISL2020-151.pdf

Refice A., Spalluto L., Bovenga F., Fiore A., Miccoli M.N., Muzzicato P., Nitti D.O., Nutricato R., Pasquariello G. (2019) – *Integration of persistent scatterer interferometry and ground data for landslide monitoring: the Pianello landslide (Bovino, Southern Italy).* Landslides, 16, pp. 447-468.

Turner A.K. (2018) – *Social and environmental impacts of landslides.* Innovative Infrastructure Solutions, 3, n. 70, 25 pp.

Urciuoli G., Comegna L., Di Maio C., Picarelli L. (2016) – *The Basento Valley: a natural laboratory to understand the mechanics of earthflows.* Rivista Italiana di Geotecnica, 1, pp. 14-33.

Vassallo R., Di Maio C., Comegna L., Picarelli L. (2012) – *Some considerations on the mechanics of a large earthslide in stiff clays.* Proc. 11th Int. Symposium on Landslides and Engineered Slopes, Banff, Canada, Taylor & Francis Group, 1, pp. 963-968.

Vassallo R., Grimaldi G., Di Maio C. (2015) – *Pore pressures induced by historical rain series in a deep-seated clayey landslide: 3D modeling.* Landslides, 12, n. 4, pp. 731-744.

Vassallo R., Grimaldi G.M., Di Maio C., Di Nocera S. (2016) – *An earth flow in structurally complex formations of the Italian Southern Apennines: geological structure and kinematics.* Proc. 12th Int. Symposium on Landslides, Naples, CRC Press, 3, pp. 1979-1986.

Vassallo R., Mishra M., Santarsiero G., Masi A. (2019) – *Modeling of landslide-tunnel interaction: the Varco d'Izzo case study.* Geotechnical and Geological Engineering, 37, pp. 5507-5531.

Vassallo R., Calcaterra S., De Rosa J., Di Maio C., Gambino P. (2020) – *Long-term displacement monitoring of two very slow earthflows by inclinometers, GPS and Cosmo-SkyMed data.* Geosciences, 10, 171.

Wasowski J., Bovenga F. (2014) – *Investigating landslides and unstable slopes with satellite multi temporal interferometry: current issues and future perspectives.* Engineering Geology, 174, pp. 103-138.

Monitoraggio di lungo periodo in situ e satellitare di due colate di terreni argillosi dell'Appennino meridionale e delle strutture su di esse costruite

Sommario

In questo articolo si riportano i risultati di un monitoraggio di lungo termine degli spostamenti di due colate in formazioni argillose tettonizzate dell'Appennino meridionale, attualmente in fase molto lenta o estremamente lenta. I movimenti delle frane, cumulandosi nel corso degli anni, hanno provocato significativi dissesti agli edifici e alle infrastrutture viarie, con importanti costi sociali ed economici. Spostamenti profondi e superficiali e pressioni interstiziali sono monitorati dal 2005; in alcune zone del versante, il monitoraggio degli spostamenti è iniziato circa 30 anni fa mediante misure inclinometriche. Grazie alle misure a terra, la cinematica delle frane è stata sufficientemente compresa. Il monitoraggio tramite interferometria satellitare sarebbe quindi molto utile per estendere nel tempo e nello spazio la conoscenza del campo di spostamenti del versante. Tuttavia, tale monitoraggio non è semplice da realizzare, sia per la direzione prevalentemente N-S degli spostamenti sia per la limitata presenza di elementi riflettori. Per minimizzare i problemi di interpretazione delle misure, sono stati analizzati in dettaglio i dati satellitari relativi alle zone in cui sono già noti gli spostamenti e le loro direzioni in quanto derivati da misure inclinometriche e GPS. Il confronto fra i dati da terra e da remoto ha infatti consentito di giungere a un'interpretazione affidabile dei risultati delle misure da remoto in un'area ampia. Inoltre, le immagini acquisite dal sistema satellitare COSMO-SkyMed, integrate con dati ERS ed Envisat (disponibili dal 1993), hanno consentito di ricostruire la storia cinematica dell'area urbanizzata anche in punti dove erano disponibili soltanto brevi serie di dati di spostamento derivanti da misure inclinometriche o dove tali misure erano assenti. I risultati dell'elaborazione hanno anche consentito di ottenere indicazioni sull'efficacia degli interventi di stabilizzazione realizzati nell'area.